

N O T I C E

THIS DOCUMENT HAS BEEN REPRODUCED FROM
MICROFICHE. ALTHOUGH IT IS RECOGNIZED THAT
CERTAIN PORTIONS ARE ILLEGIBLE, IT IS BEING RELEASED
IN THE INTEREST OF MAKING AVAILABLE AS MUCH
INFORMATION AS POSSIBLE

81-10154

CR-164268

"Made available under NASA sponsorship in the interest of early and wide dissemination of Earth Resources Survey Program information and without liability for any use made thereof."

DRYLAND PASTURE AND CROP CONDITIONS AS SEEN BY HCMM

FINAL REPORT

Prepared for
NASA-Goddard Space Flight Center
Greenbelt, Maryland 20771

Contract NAS5-24383

(E81-10154) DRYLAND PASTURE AND CROP
CONDITIONS AS SEEN BY HCMM Final Report
(Texas A&M Univ.) 63 p HC A04/MF A01

N81-24492

CSCL 08E

Unclass

G3/43

00154



**TEXAS A&M UNIVERSITY
REMOTE SENSING CENTER**
COLLEGE STATION, TEXAS



RECEIVED

APR 27 1981

SIS/902.6
Hcm-049
Type III
Final

Progress Report RSC 3712-12

DRYLAND PASTURE AND
CROP CONDITIONS AS
SEEN BY HCMM

Original photography may be purchased from
EROS Data Center

by

Steve Egan, et al.

57198

W. D. Rosenthal, J. C. Harlan (P. I.), and
B. J. Blanchard

Remote Sensing Center
Texas A&M University

Final Report

Prepared for

NASA - Goddard Space Flight Center
Greenbelt, Maryland 20771

PREFACE

The primary objective of this project was threefold:

1. to assess the capability for determining canopy temperatures in dryland farming regions from HCMM data,
2. to assess the capability for determining soil moisture (antecedent precipitation index) in dryland crops from HCMM data, and
3. to determine the relationship of HCMM-derived soil moisture (antecedent precipitation index--API) and canopy temperatures with the condition of winter wheat and dryland farmlands during the principal growth stages.

These goals were to be accomplished primarily in three ways:

1. thermal (HCMM and aircraft) parameters of soil moisture and crop canopy temperatures were to be derived,
2. a technique was to be developed to calculate the antecedent precipitation indices from the thermal parameters of soil moisture and canopy temperatures, and
3. an input parameter for yield models was to be developed.

Aircraft (M²S) and ground data was collected in May 1978 over the Washita Watershed area in central Oklahoma. Techniques developed from the aircraft flights were then applied to HCMM data analysis.

Results from the flight indicated that (1) canopy temperatures were accurately measured remotely, (2) pasture temperatures indicated pasture and wheat moisture conditions, (3) no relationship could be developed with that set of data between wheat yield and thermal infrared data due to a lack of moisture stress during the measurement period, and (4) lake surface temperature data was useful in normalizing thermal IR data.

Later, initial HCMM day IR data alone indicated thermal gradients were related to corresponding precipitation gradients (i.e., the August 15 storm in western Kansas). Since precipitation was an input into antecedent precipitation index, we believed day/night or day/day temperature differences would be related to antecedent precipitation index conditions in areas as small as 5 km. Day/day relationships were analyzed because many night IR scenes had an excessive amount of cloud cover.

Day/night surface temperature differences for a storm over the watershed in October, 1978, was strongly related ($R^2=.76$) to API conditions for approximately a seven-day period following precipitation. The relationship deteriorated after this period, due to other factors dominating thermal variability across the image.

Day/day temperature differences from HCMM data collected before and after a storm in July 1978 were also strongly related ($R^2=0.68$) to API conditions. Again the relationship deteriorated after a 7-day period after the storm.

Comparisons of the two techniques for a storm in October showed both to estimate API conditions equally well.

As a result of our study, we found 1) canopy temperatures were accurately measured remotely, 2) pasture surface temperature differences detected relative soil moisture (API) differences, 3) pasture surface temperatures were related to stress in nearby wheat fields, and 4) no relationship was developed between final yield differences, thermal infrared data, and soil moisture stress at critical growth stages due to a lack of satellite thermal data at critical growth stages. The HCMM thermal data proved to be quite adequate in detecting relative moisture differences; however, with a 16-day day/night overpass frequency, more frequent overpasses are required to analyze more cases within a 7-day period after the storm. In addition, better normalization techniques are required if day/day temperature differences will be analyzed further.

ACKNOWLEDGEMENTS

We are deeply indebted to the personnel at the Southern Great Plains Hydrology Lab at Chickasha, Oklahoma. They provided valuable ground data used in analyzing aircraft and HCMM data. In particular we would like to thank Mr. Gerald Coleman for his valuable assistance and cooperation.

We have enjoyed extraordinary cooperation from the individuals at NASA/GSFC associated with our HCMM project, and are very grateful to them for their help, guidance and communication. We wish to thank, especially, John Price, Locke Stuart and Dick Stonesifer of NASA, and Ralph Peterson of GE.

TABLE OF CONTENTS

	Page
Introduction.	1
Objectives and Tasks.	3
Antecedent Precipitation Index (API).	4
Site Description.	4
Aircraft Flight Data Handling	6
Emissivity Measurement Procedure10
Aircraft Results.12
HCMM Image/Data Analysis.21
Surface Temperature/Precipitation Relationships.22
Day/Night Registered Data vs. API.26
Day/Day Temperature Differences vs. API.32
Comparison of the Two Techniques45
Conclusions51
Bibliography.53

LIST OF ILLUSTRATIONS

		Page
Figure 1	A plot of K for 30 cm depth as a function of time.5
Figure 2	The geologic distribution across the Washita Watershed area.7
Figure 3	Location of the two flight lines flown in May 1978.8
Figure 4	Computer greymap of the afternoon flight over several pasture (light tones) and wheat fields (dark tones) . .	17
Figure 5	Day/night temperature differences along both flight lines versus API ($R^2=0.10$)	19
Figure 6	Day/night temperature differences on May 8/9, 1978 versus concurrent volumetric soil moisture content ($R^2=0.10$)	20
Figure 7	A 1:250,000 rainfall contour map of the storm over the Colby, Kansas area.	23
Figure 8	Thermal infrared greymap of the same area as described in Figure 7	24
Figure 9	Thermal IR greymap (August 15, 1978) of the area near Garden City, Kansas (point A)	25
Figure 10	Washita Watershed raingage sites.	28
Figure 11	Day/night temperature difference greymap of the Washita Watershed area for October 16 and 17.	30
Figure 12	Oct. 16/17 day/night temperature differences versus API conditions ($R^2=0.25$)	31
Figure 13	October 12 day IR greymap, the southern part of the watershed was not included with the digital data.	33
Figure 14	October 15 night IR greymap of the Washita Watershed area.	34
Figure 15	October 12/15 day/night temperature differences versus API conditions ($R^2=0.76$)	35
Figure 16	Rainfall contour map of the July 21, 1978 storm which passed over parts of the watershed area	36

List of Illustrations (cont.)

	Page
Figure 17	Thermal IR greymap of the Washita Watershed area on July 13, 1978. 38
Figure 18	Thermal IR greymap of the Washita Watershed area on July 24, 1978 40
Figure 19	Thermal IR greymap of the Washita Watershed area on July 29, 1978 41
Figure 20	Surface temperature and API as a function of distance along the transect A-B on July 24, 1978. 42
Figure 21	Surface temperatures and API as a function of distance along the transect A-B on July 29, 1978. 43
Figure 22	July 24/July 13 day/day temperature differences versus API conditions on July 24 ($R^2=0.68$). 44
Figure 23	July 29/July day/day temperature differences versus July 29 API ($R^2=0.25$). 46
Figure 24	Thermal IR greymap of the Washita Watershed area on August 31, 1978 48
Figure 25	October 12/August 31 day/day temperature differences versus API differences between the same two dates ($R^2=0.57$). 49
Figure 26	October 17/August 31 day/day temperature difference versus API differences between the same two dates ($R^2=0.43$). 50

LIST OF TABLES

	Page
Table 1	Soil moisture data collected at Chickasha on 5/9/78. 13
Table 2	Emissivity of Oklahoma sites. 15
Table 3	Day/night surface temperature data. 18
Table 4	Raingage sites eliminated for having less than 60% pasture in the surrounding 1 sq. km 29

INTRODUCTION

Soil moisture estimation has become an important input into various agricultural models--yield, water budget, etc. The difficulty has arisen in obtaining accurate estimations over large areas. If normal techniques, such as gravimetric and neutron probe, are used many samples are required. Use of thermal infrared information is one technique recently implemented to analyze soil moisture stress and reduce the number of samples. A series of experiments has related field moisture stress to crop/air temperature differences (Jackson, et. al., 1977). Their ground studies have encouraged more interest in the thermal relationship with soil moisture stress (Gardner, 1979). Their applications have primarily been on the ground.

For satellite thermal IR data to be useful another thermal parameter sensitive to soil moisture content needs to be analyzed. Thermal inertia, which is a function of day/night temperature differences, is theoretically related to soil moisture content (Geiger, 1950). This variable was one of the principal variables to be analyzed when HCMM was launched.

The satellite was launched in 1978 as a research satellite to evaluate the utility of satellite thermal infrared data in areas such as geology, hydrology and agriculture. For HCMM to be useful in soil moisture analysis, large fields were required. In many areas of the world commercial fields are quite small and large stress "indicator" fields are needed. Landsat has shown pasture areas, which often are quite large, to be indicative of environmental changes (Harlan

et.al., 1978). We therefore wanted to evaluate the thermal infrared response of pasture and relate it to soil moisture stress as detected from HCMM in nearby cash-crop fields.

OBJECTIVES AND TASKS

Our primary objective was threefold:

- 1) to assess the capability for determining canopy temperatures in dryland farming regions from HCMM data.
- 2) to assess the capability for determining soil moisture (antecedent precipitation index) in dryland crops from HCMM data.
- 3) to determine the relationship of HCMM-derived soil moisture (antecedent precipitation index) and canopy temperature values with the condition of winter wheat and dryland farmlands during the principal growth stages.

These goals were to be accomplished primarily in threeways: -

- 1) thermal (HCMM and aircraft) parameters of soil moisture and crop canopy temperatures were to be derived,
- 2) a technique was to be developed to calculate the antecedent precipitation indices from the thermal parameters of soil moisture and canopy temperatures, and
- 3) an input parameter for yield prediction models was to be developed.

The first procedure was to collect aircraft thermal infrared and soil moisture data. Data were compared and techniques developed from the aircraft flights and these then were applied to HCMM thermal/soil moisture relationships.

ANTECEDENT PRECIPITATION INDEX (API)

As mentioned in the objectives, the primary soil moisture parameter to be used was antecedent precipitation index. It is a relatively simple variable with daily precipitation as the only input. Blanchard (1978) developed the model for the Washita River Watershed area as given in equation (1).

$$API_i = (API_{i-1} * K) + p0.829 \quad (1)$$

where API_i and API_{i-1} are respectively, present and previous day's antecedent precipitation index values (cm), K is a dimensionless parameter dependent on the thickness layer of interest and time of year, and P is the daily precipitation rate (cm). The constant, K , differs between watersheds due to different vegetative and topographic characteristics. K for a 30 cm depth--the depth of interest in our study area--varies from 0.98 to 0.84 during the year (Figure 1). The equation has been used by hydrologists to empirically estimate soil moisture depletion and to evaluate potential runoff conditions for a given storm. API and volumetric soil moisture are similar, because API under drying conditions parallels the soil moisture decrease.

SITE DESCRIPTION

To obtain a large soil moisture (API) data set, a dense network of raingages was needed. The area chosen was the Washita Watershed area in central Oklahoma. The watershed had one raingage every 30

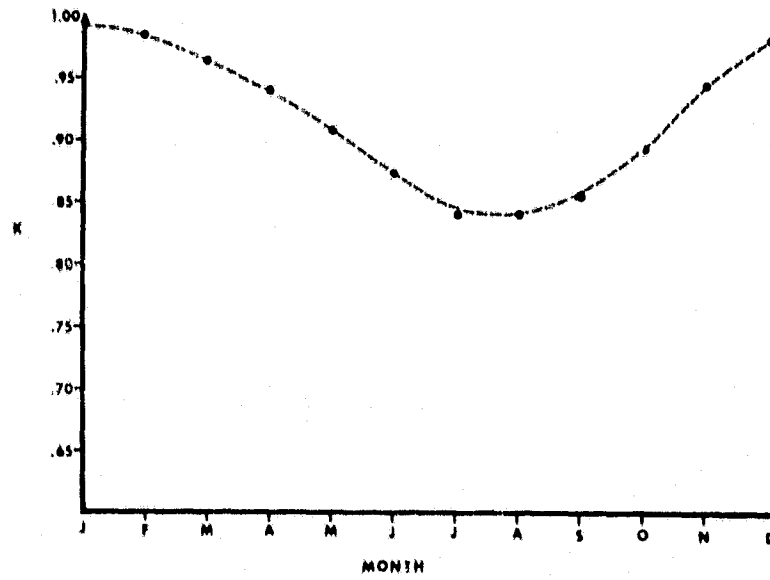


Figure 1. A plot of K for a 30 cm depth as a function of time

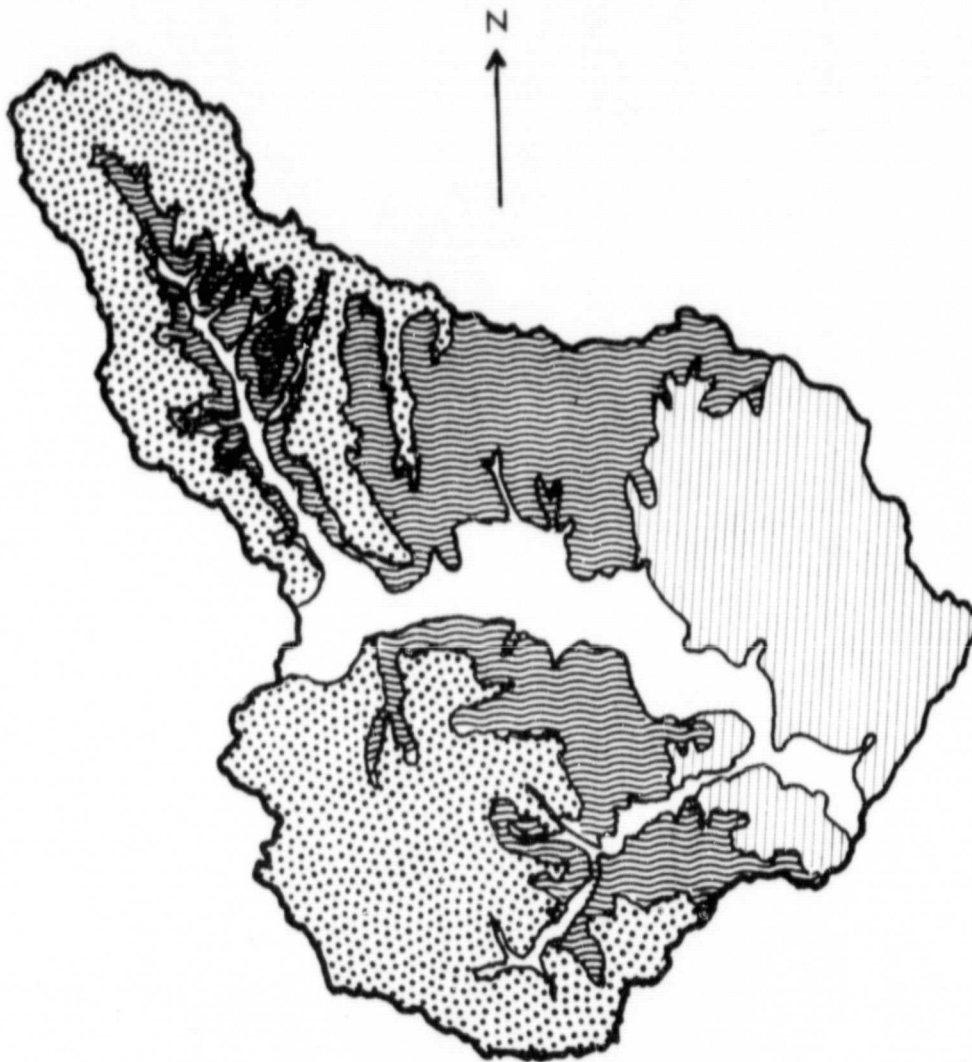
square kilometers. Precipitation data was collected daily in 1978 at 168 raingages throughout the watershed. The 65 km distance from east to west across the watershed covered a 15 cm range of annual rainfall (70-85 cm)(NOAA, 1980). The area was interspersed with pasture and crops (primarily dryland winter wheat). Only a few irrigated fields were in the western area of the watershed. A wide range of soil types--sandy to clay--also prevailed across the watershed. Such differences are likely to reflect soil moisture differences. The soil type differences were attributed directly to geologic formations in the area (Figure 2).

AIRCRAFT FLIGHT DATA HANDLING

As described in the "Objectives and Tasks" section, thermal IR data was to be collected from the NASA C-130. The purpose of the aircraft flight over the Washita Watershed was threefold: to prove if

- 1) canopy temperatures could be measured remotely
- 2) pasture temperature differences were related to regional soil moisture stress, and
- 3) temperature differences in pasture were related to soil moisture stress in dryland wheat at approximately heading growth stage,

To accomplish the purpose, we selected flightlines over two areas of the watershed--one in a clay loam area and the other in a sandy alluvium (Figure 3). The flights were scheduled during May 1978--a period when wheat has usually headed and is sensitive to moisture stress (Robins and Domingo 1962).






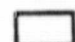
-  Sandstone
-  Shale & Gypsum
-  Shale & Sandstone
-  Alluvium

Figure 2. The geologic distribution across the Washita Watershed area

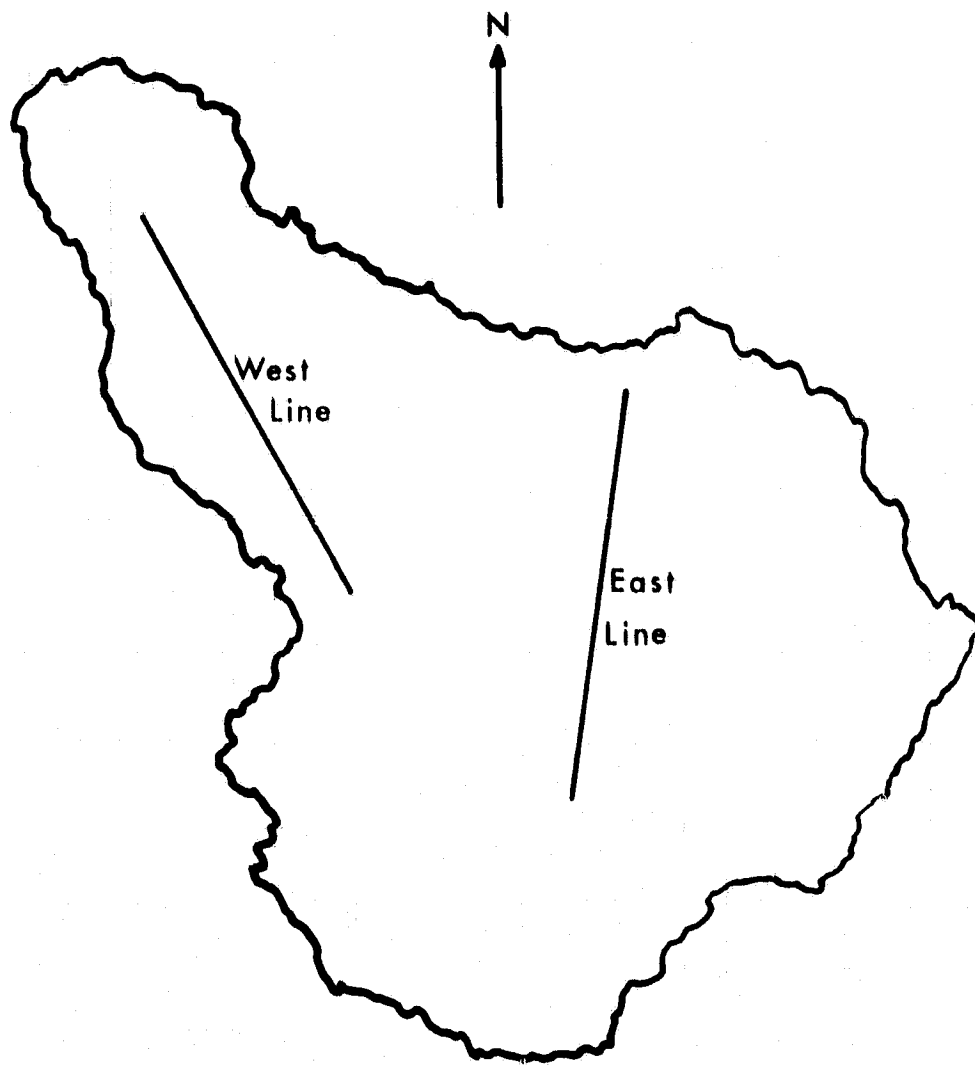


Figure 3. Location of the two flight lines flown in May 1978

About one month before the scheduled flight, commercial fields were selected for measurement. To eliminate drastic soil type differences from affecting the analysis, as many adjacent pasture and wheat fields were selected as was possible. Permission was granted by farm operators to sample in 16 fields. One representative site within each of the fields was selected for intensive measurement. Each site area was approximately 50 feet in diameter.

To compare aircraft thermal data between pasture and wheat, three types of ground level measurements were collected: (1) gravimetric soil moisture at each site; (2) surface temperature of a nearby lake and (3) thermal emissivity data at each site. Six to eight gravimetric samples were collected for the two 15-cm thick increments (0-15 cm and 15-30 cm). This technique was the most accurate method available, within the limitations of time available and the number of samples needed. Utilizing the high thermal emissivity and heat capacity of water, lake surface temperatures were used to calibrate the M²S thermal data. The lake temperatures were collected in conjunction with the aircraft overpass. Emissivity measurements were collected at each site to determine the influence emissivity differences between pasture and wheat had on surface temperature differences. One measurement was collected at an area representative of the vegetative cover at a given site. The technique was similar to that used by Fuchs and Tanner (1966) and is described in the following section.

Emissivity Measurement Procedure

The procedure to determine emissivity of a surface consisted of five basic measurements using a radiation thermometer (in this case a Barnes Instatherm): (1) the temperature of a known-emissivity panel exposed to the sun; (2) the temperature of the panel covered by a large can lined with aluminum foil; (3) the temperature of the vegetated surface exposed to the sun; (4) the temperature of the surface after shading from the sun; and (5) the temperature of the surface covered by the foil-lined can.

After placing the panel horizontally on the ground, and allowing the panel temperature to equilibrate, panel temperatures were collected. By standing far from the panel, the portion of the sky blocked by the operator and instrument was minimized. In any case, the operator and instrument was in the same position relative to the target and sun during all measurements. The response measured by the thermometer (R_{panel}) is given by

$$R_{\text{panel}} = F(T)[\sigma T^4 \epsilon_{\text{panel}} + (1 - \epsilon_{\text{panel}}) B_s]. \quad (2)$$

where $F(T)$ is the integrated spectral response of the instrument over all wavelengths, B_s is the background thermal radiation, ϵ is thermal emissivity, and T is the radiative temperature.

Immediately after this measurement, the foil-lined can, with the thermometer mounted on it looking through a hole in the closed end, was placed over the plate. The plate temperature was read immediately, before the temperature began to decrease. The temperature as measured by the radiometer was related to actual temperature by

$$R_{cp} = F(T)\sigma T_{panel}^4 \quad (3)$$

where R_{cp} is the radiation received by the instrument with the can placed over the panel.

Comparing these two results, we calculated $F(T)B_s$. The plate measurements were taken once at each site--more frequently if the sky was partly cloudy, as background radiation, B_s , is a function of water vapor concentration and cloud over.

Next, a large representative area of the surface was shaded using the panel or other large opaque object. The temperature of the shaded area was monitored until the surface temperature stabilized with the surroundings (this took approximately 3-5 minutes). By shading the area, direct solar radiation was eliminated and temperature eventually stabilized for the can measurement. The shaded surface temperature $(T)_{surface}$ as measured by the instrument was related to the instrument response by

$$R_{surface} = F(T)[\epsilon\sigma T_{surface}^4 + (1-\epsilon)B'_s] \quad (4)$$

where B'_s is approximately equal to B_s . Any difference between B_s and B'_s is due to the thermal radiation emitted from the shade.

While keeping the area shaded, the can with the thermometer mounted on it was placed over the area and the surface temperature was recorded immediately. It was important that this measurement be taken within 10 seconds of covering the surface because the shaded canopy temperature was likely to change. The response from the thermometer was a direct function of the actual surface temperature:

$$R_{CS} = F(T)\sigma T^4_{\text{surface}} \quad (5)$$

where R_{CS} is the radiation received by the thermometer when the can was placed over the surface.

Since we are given $F(T)B_s$, T , and R_{surface} from the previous measurements, we calculated ϵ of the given surface using the equation

$$\epsilon = \frac{R_{\text{surface}} - F(T)B_s}{R_{CS} - F(T)B_s} \quad (5)$$

The calculated ϵ from equation 5 was the actual ϵ because $F(T)$ was a factor in R_{surface} , R_{CS} , and $F(T)B_s$ and consequently cancelled out.

AIRCRAFT RESULTS

The aircraft flew at 5,000 feet over the selected fields on May 8 and 9, 1978; ground data was collected on May 9. Rains during the previous week supplied the soil with adequate moisture. No moisture stress symptoms were observable. Wheat fields at this time of the year were approximately 75 cm tall and heading. Most of the pasture fields had vegetation less than 15 cm tall. All of the fields, except for one bare field and one grazed wheat field, had greater than 50% ground cover.

The volumetric moisture content within the top 30 cm at each site is shown in Table 1. From the results:

- (1) fields were drier along the west than east flight line, and

Table 1: Soil Moisture Data Collected at Chicasha on 5/9/78

<u>East Flight Line Site</u>	<u>Depth (cm)</u>	<u>Moisture (% by volume)</u>	<u>West Flight Line Site</u>	<u>Depth (cm)</u>	<u>Moisture (% by volume)</u>
E-1 (wheat)	0-15 15-30	28.8 25.9	W-1 (pasture)	0-15 15-30	26.7 27.0
E-2 (wheat)	0-15 15-30	26.4 20.9	W-2 (pasture)	0-15 15-30	22.9 17.8
E-3 (pasture)	0-15 15-30	25.7 22.9	W-3 (wheat)	0-15 15-30	15.1 13.8
E-4 (wheat)	0-15 15-30	19.8 17.2	W-4 (pasture)	0-15 15-30	17.5 17.6
E-5 (wheat)	0-15 15-30	31.8 31.2	W-5 (wheat)	0-15 15-30	14.4 13.8
E-6 (pasture)	0-15 15-30	26.2 24.8			
E-7 (wheat)	0-15 15-30	29.9 26.5			
E-8 (wheat)	0-15 15-30	23.4 26.7			
E-9 (bare soil)	0-15 15-30	29.2 31.4			
E-10 (pasture)	0-15 15-30	30.0 34.6			
E-11 (wheat)	0-15 15-30	30.1 30.1			

(2) pasture fields along the west flight line were wetter than dryland winter wheat fields.

The soil moisture difference between the flight lines was partly due to water-holding capacity differences of the two soil types along each flight line. Fields along the east flight line are in clay loam; along the west flight line, in a sandy loam which holds less moisture.

Due to differences in the amount of green material, the pastures were wetter than the wheat fields along the west line. Most of the pastures averaged from 50-80% green material, while wheat averaged from 90-100% green material. The larger biomass transpired more water and depleted the soil water content faster.

No significant difference between pasture and wheat thermal emissivity was detected (Table 2). The reason was that thermal emissivity appeared to be based primarily on the amount of vegetative cover within the scene rather than the type of cover. Most of the fields had similar crop cover in terms of the sensitivity of emissivity. Consequently, emissivity differences had no effect on comparing wheat and pasture temperature differences.

Lake surface temperatures as measured on the ground were 20°C at the pre-dawn time (3 a.m. CDT), and 21°C during the afternoon (2 p.m. CDT), reflecting the small diurnal variation in lake temperature due to its high heat capacity.

Upon arrival of the M²S data at TAMU, the digital thermal data was converted to surface temperatures, scaled, and transferred to a magnetic tape (CCT). The range of digital data on the magnetic tape

Table 2: Emissivity of Oklahoma Sites

East Flight Line		West Flight Line	
E - 1	(wht.) .99	W - 1	(past.) .97
- 2	(past.) .99	- 2	(past.) .98
- 3	(past.) .97	- 3	(wht.) .97
- 4	(wht.) .97	- 4	(past.) .96
- 5	(wht.) .99	- 5	(wht.) .97
- 6	(past.) .91		
- 7	(wht.) .99		
- 8	(wht.) .92		
- 9	(bare soil) .92		
-10	(past.) .99		
-11	(wht.) .97		

was 0-225. With this maximum range the digital data was scaled by adding or subtracting a given constant so the complete range of surface temperatures fell into the 0-255 range. The range of temperatures on a given file were then separated into 8 regions, each assigned a greytone, and printed out as a greymap. One pixel corresponded to an area on the ground approximately 11 feet in diameter. Each grey tone corresponded to approximately 1°C range. Figure 4 gives an example of the greymap of site 4 along the west flight line. From the greymap, surface temperatures were averaged and within-field variability evaluated at each ground measurement site.

The thermal IR data collected proved to be close to actual surface temperatures (within 2°C), as determined by comparing aircraft lake temperatures to actual lake surface temperatures. Therefore, lake surface temperatures may be used as a normalization technique for HCMM thermal IR data.

Day/night site surface temperature differences ranged from 7 to 18°C (Table 3). The day/night temperature relationships between API and volumetric soil moisture were very similar (Figures 5 and 6). In both cases, a general relationship is apparent with some scatter ($R^2 = .10$). However, the wheat canopy temperatures varied more than pasture temperatures. The variability was likely due to other growth factors (nutrient deficiencies, canopy cover, etc.) affecting growth and canopy temperatures. Since moisture stress was not evident, final wheat yields were consistent along both flight lines, consequently, yield differences were not apparent through thermal



Figure 4. Computer greymap of the afternoon flight over several pasture (light tones) and wheat fields (dark tones)

Table 3: Day/Night Surface Temperature Data

<u>Site</u>	<u>Day Temp.</u>	<u>Night Temp.</u>	<u>Day-Night Diff.</u>
E-1 (wheat)	25.06°C	17.32°C	7.74°C
E-2 (oats-pasture)	27.96°C	15.98°C	11.98°C
E-3 (pasture)	30.31°C	16.12°C	14.19°C
E-4 (wheat)	25.52°C	16.96°C	8.56°C
E-5 (irr. wheat)	24.33°C	15.77°C	8.56°C
E-6 (pasture)	30.49°C	16.68°C	13.81°C
E-7 (wheat)	23.33°C	17.25°C	6.08°C
E-8 (wheat-graze)	27.26°C	16.46°C	10.80°C
E-9 (bare)	32.06°C	15.11°C	16.95°C
E-10 (pasture)	32.90°C	16.05°C	16.85°C
E-11 (wheat)	27.82°C	17.11°C	10.71°C
W-1 (pasture)	31.81°C	15.57°C	16.24°C
W-2 (pasture)	34.01°C	15.44°C	18.57°C
W-3 (wheat)	24.92°C	16.31°C	8.61°C
W-4 (pasture)	33.26°C	15.74°C	17.52°C
W-5 (wheat)	25.64°C	16.04°C	9.60°C
Lake	20.61°C	22.42°C	-1.81°C

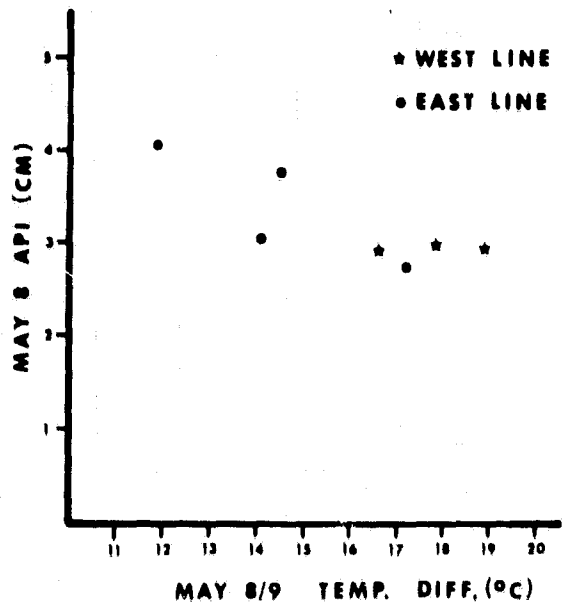


Figure 5. Day/night temperature differences along both flight lines versus API ($R^2=0.10$)

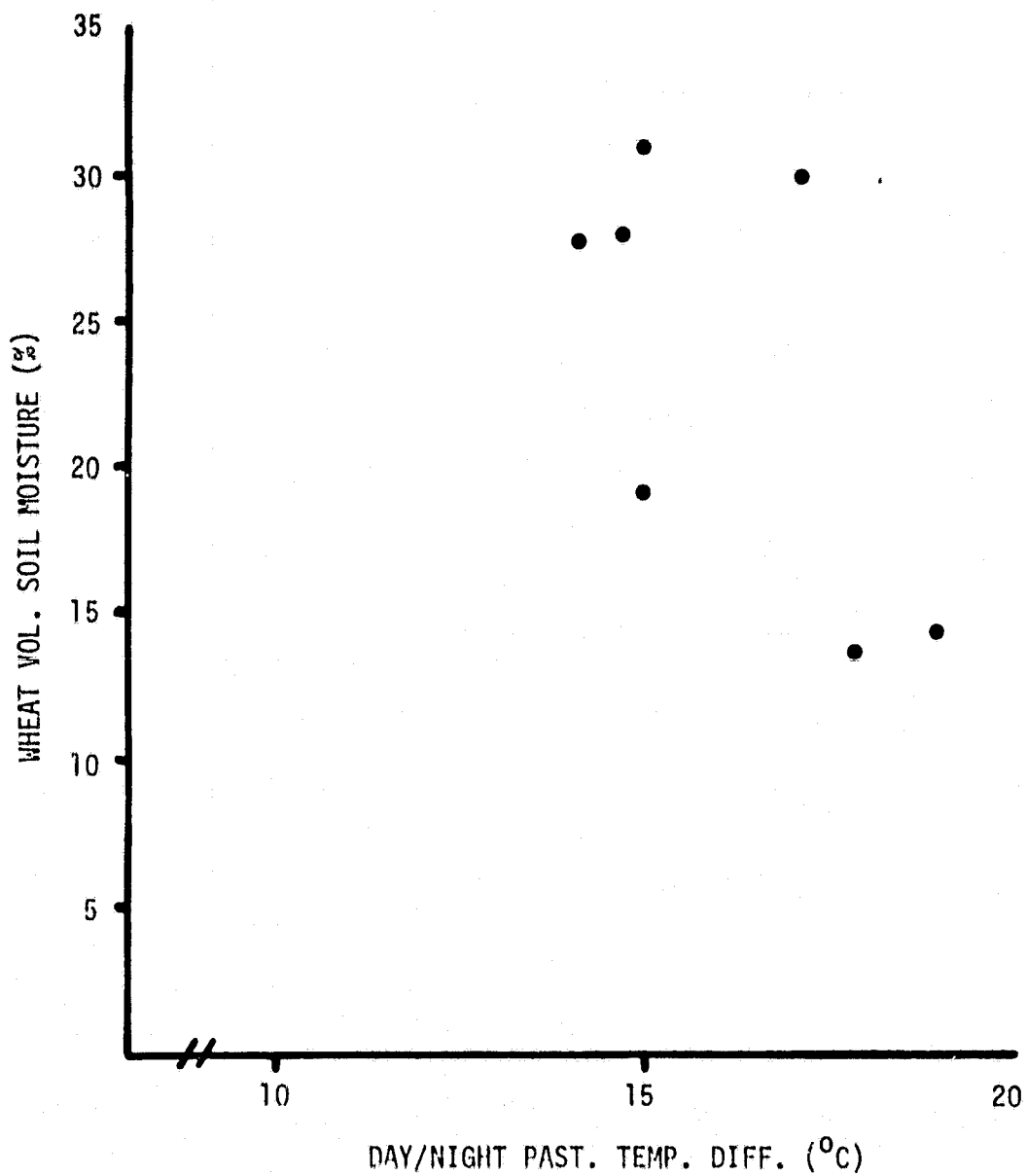


Figure 6. Day/night temperature differences on May 8/9, 1978, versus concurrent volumetric soil moisture content ($R^2=0.10$).

differences at heading stage. Therefore the third purpose of the aircraft flight could not be fulfilled.

In summary, results from the flights indicated that (1) canopy temperatures were accurately measured remotely, (2) pasture temperatures indicated regional pasture and wheat moisture conditions.

HCMM IMAGE/DATA ANALYSIS

Data analysis

Upon arrival of HCMM data in CCT form, the watershed area was located using a DCD (digital color display). The DCD also provided a quick means of analyzing the quality of the thermal data. All of the HCMM thermal data was of excellent quality (visible channel data analysis was not part of this project). Once the areas had been located on the tape (CCT), a greymap was produced. The greymap software permitted variable sized pixels, thus allowing for different scale maps to be produced, as needed. The software also separated the data into eight increments as described in the previous section. Documentation of the greymap software is available on request.

Topographic maps and greymaps at 1:250,000 scale were then used to locate raingage sites through the watershed. Registration accuracies appeared to be within 1 pixel (.25 square kilometers). Surface temperatures were then thematically compared with soil moisture (API) or with temperatures of the same area on a different date. Variations of the technique in analyzing surface temperatures are described in detail in later sections.

Surface Temperature/Precipitation Relationships

Several HCMM passes were noteworthy with respect to precipitation and API. For example, a storm passed over two areas in western Kansas--Colby and Garden City--early on August 15. Same-day HCMM (ID A-A0111-2080) CCT data was ordered and analyzed. Surface temperatures for 1 sq. km areas were then calculated for various sites in Western Kansas.

Near Colby, the storm dropped as much as 2.5 cm in the area, as seen in the contour map in Figure 7. As the storm traveled eastward precipitation increased. A similar pattern was evident on the thermal infrared greymap (Figure 8). The rainfall contour map area is outlined in the greymap. Surface temperatures decreased with increasing rainfall. The temperature gradient of 8.1°C corresponded to the 0-2.5 cm precipitation gradient. No definite explanation could be given as to why the river basins were warmer than the surrounding area. One possible reason was soil type differences--clay soil in the river basin having a lower thermal conductivity than sandy soil--causing warmer temperatures in the river basins. Neither could an explanation be found for the cool areas in the top part of Figure 8, where rainfall was less than 0.6 cm. Other factors affecting surface temperatures, such as land use, need to be analyzed within the area.

The storm also passed close to Garden City. The thermal pattern again closely followed the rainfall pattern (Figure 9). A 12°C temperature range was apparent in the image. Garden City is shown as 'A' on the map. The weather station at the Experiment Station,

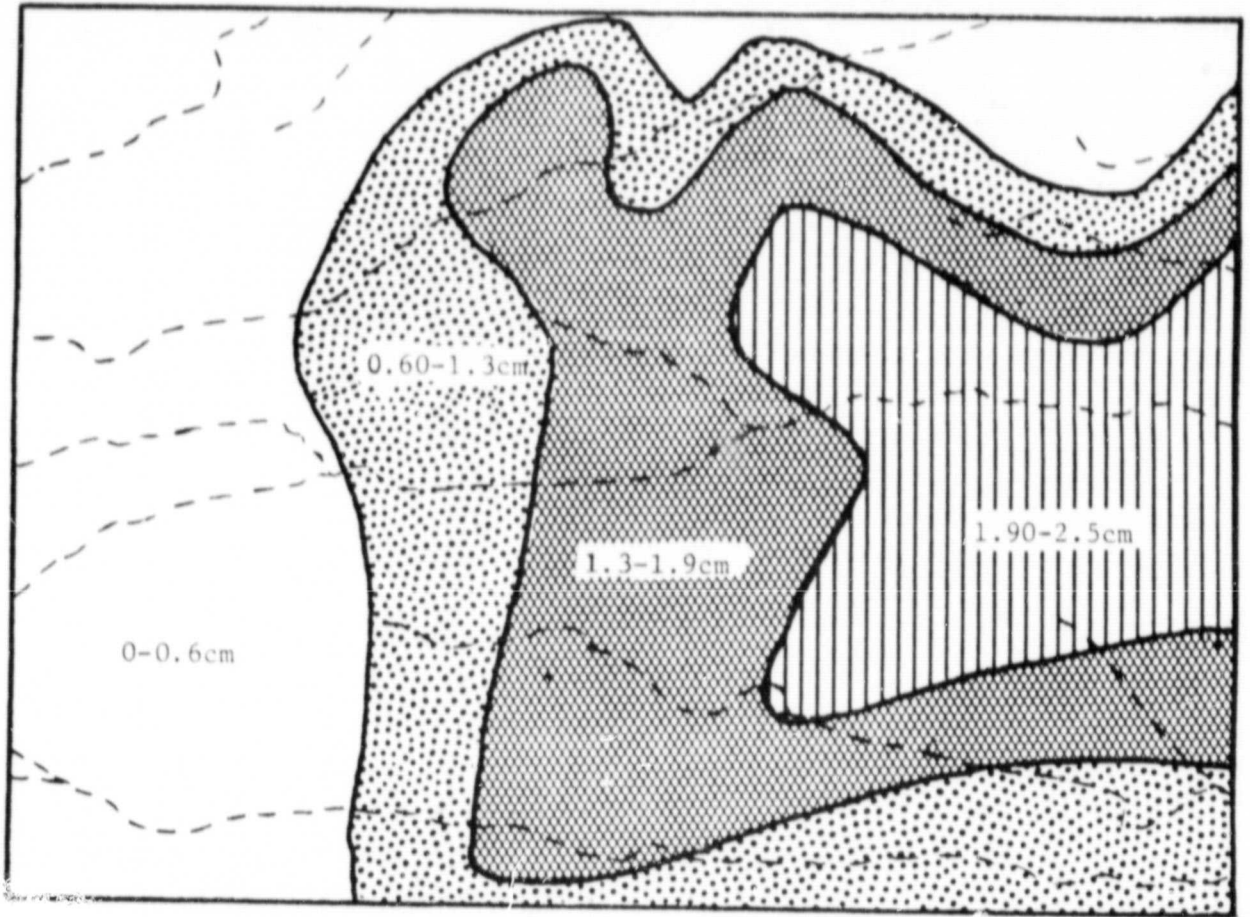


Figure 7. A 1:250,000 rainfall contour map of the storm over the Colby, Kansas area

HCYR DRY HILIST IS COLBY
USING BANDS 1 AND 1

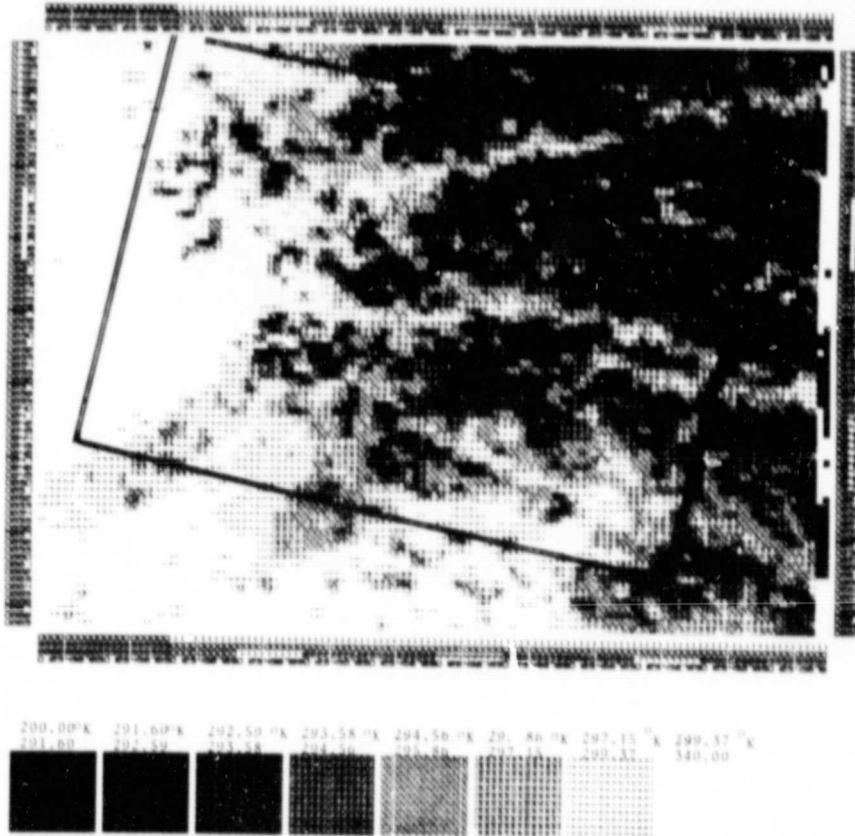


Figure 8. Thermal infrared greymap of the same area as described in Figure 7. The area is outlined on the greymap

ORIGINAL PAGE IS
OF POOR QUALITY

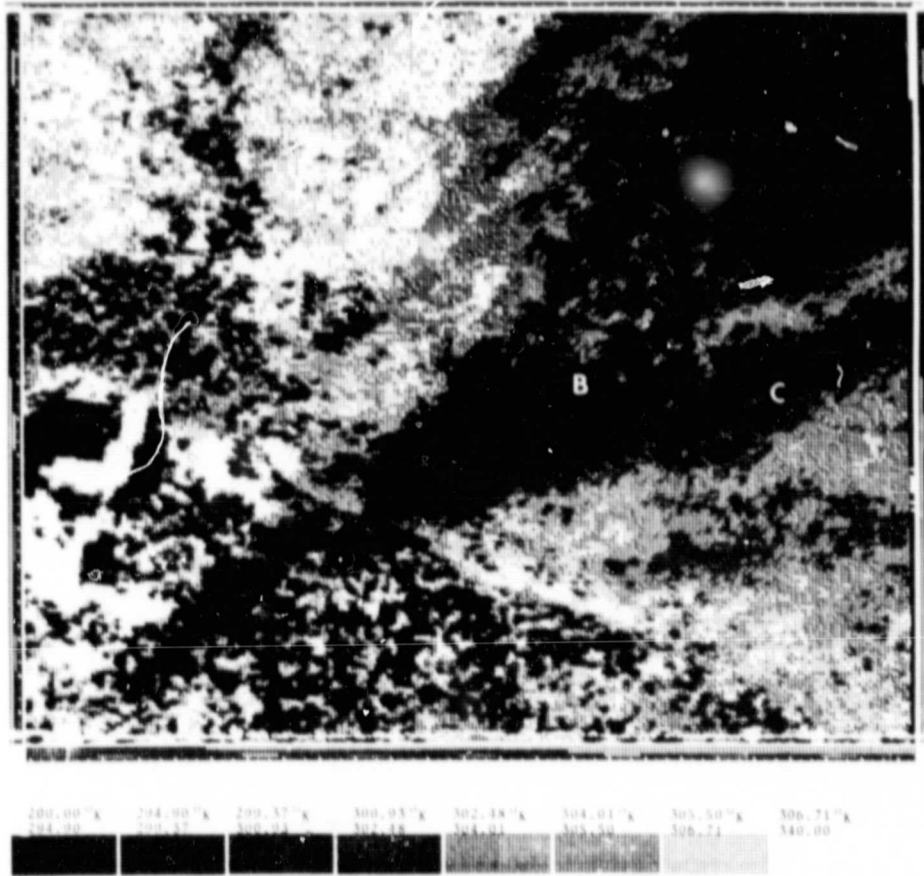


Figure 9. Thermal IR greymap (August 15, 198) of the area near Garden City, Kansas (point A)

northeast of town, received only a trace of rainfall. Kalvesta (area B on the greymap), a town 25 miles northeast of the experiment station, received 2.5 cm on the data; Jetmore (area C on the greymap) received 3.3 cm on the 15th. Note the distinct cool band which extended from southwest to northeast. The width of this band increased with distance traveled to the northeast, corresponding to the increasing size of the storm (from about 5 to 25 km). The temperature gradient corresponding to the 3.3 cm precipitation gradient was 10.6°C. Both the storm at Colby and the one at Garden City induced an 8°C temperature drop for a 2.5 cm rainfall, thus indicating that precipitation, which is a direct input to API, is directly related to daytime surface temperature. The uniform cooling through both areas indicated that vegetated and fallow fields are cooled the same amount. The coolest areas were undergoing near-potential evapotranspiration rates and warmer areas, much less than potential evapotranspiration rates (Campbell, 1979).

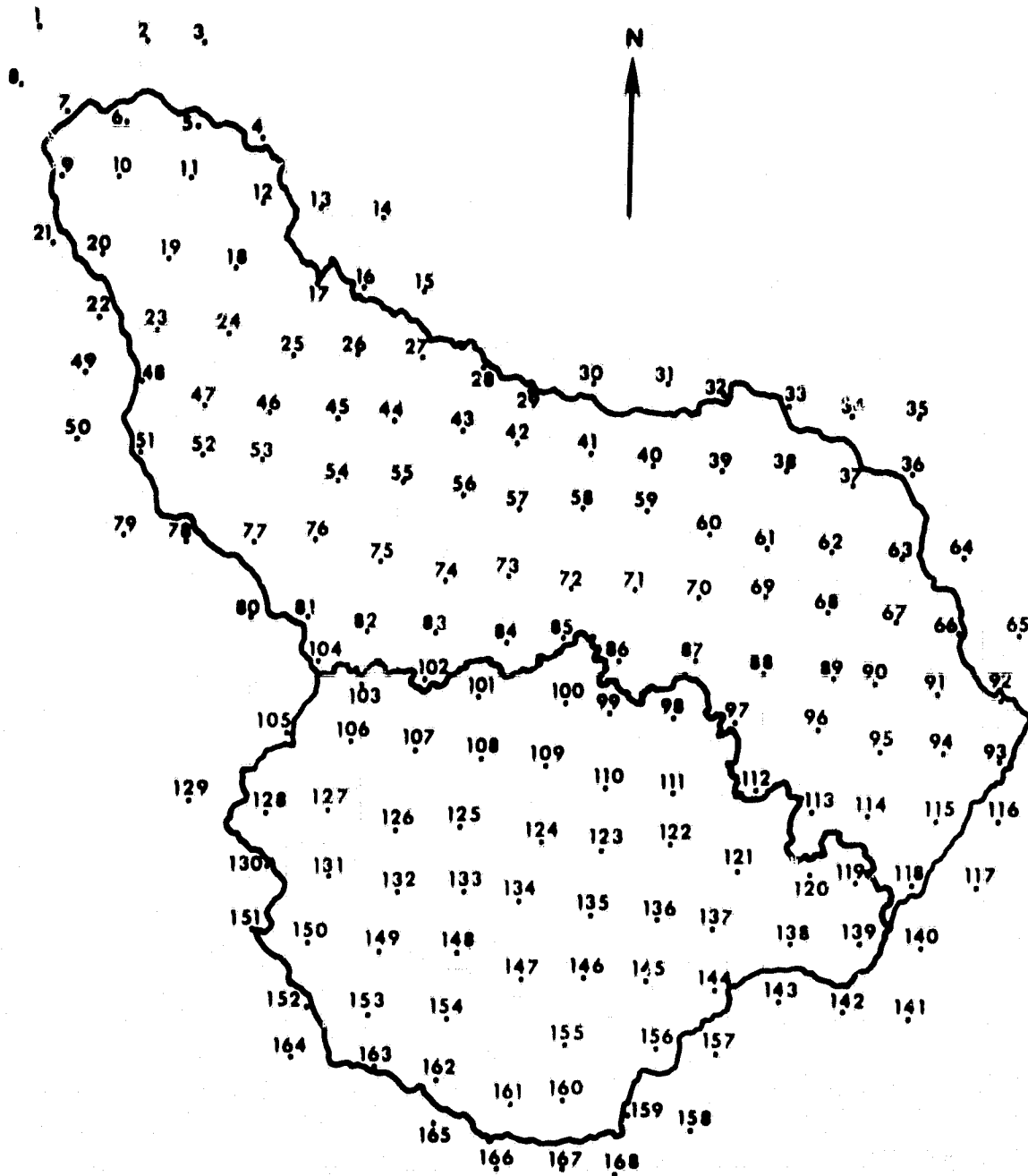
Day/Night Registered Data VS API

During the first week in October, a storm passed over the northern part of the Washita Watershed. API estimates ranged from 3 cm to 0.25 cm over the watershed during this period. Moisture conditions (API) before the storm were approximately 0.25 cm. Fortunately, HCMM collected day/night registered data on October 6 (ID A-A0163-08460, A-A0163-1970), October 11/12 (ID A-A0168-08400, A-A0169-19490), and October 16/17 (ID A-A0173-08330, A-A0174-19240). We have received and analyzed the October 16/17 data set, the other two are on order. The technique for analysis was 1) producing a

1:250,000 greymap to locate watershed raingage sites, 2) calculating the average temperature for an area 2.5 square kilometers around each raingage, 3) calibrating the average surface temperature using actual lake surface temperatures, 4) screening the IR data to include only raingage areas having greater than 60% pasture in order to diminish the thermal variability due to land use differences, and 5) plotting the day/night temperature difference at each raingage site versus API. Of the 168 raingages throughout the watershed (Figure 10), 55 raingage sites were eliminated (Table 4). The day/night temperature difference greymap indicated low differences in the northern part of the watershed (Figure 11). The low day/night temperatures were related to high API estimates (Figure 12). The coefficient of determination was 0.25, indicating that thermal inertia is not strongly related to API alone, and that other factors were affecting the relationship as well. The general relationship of high day/night temperature differences corresponding to low API, however, was still apparent. In addition, the relationship was independent of soil type.

We unfortunately were unable to receive the other two day/night registered data sets by the project end. However, we did analyze the October 12 day and October 15 night images.

The 60-hour temperature difference still indicated relative moisture differences throughout the watershed. The procedures followed were similar to the 12-hour day/night data analysis, except the 60-hour day/night images had to be manually registered at the Remote Sensing Center. Registration errors we feel were within 2



0 1 2 3 4 5 6 7 8 9
MILES

WASHITA WATERSHED RAINGAGE SITES

Figure 10

<u>Rain Gage</u>	<u>Rain Gage</u>	<u>Rain Gage</u>
1	57	102
2	62	103
3	72	104
7	73	105
8	79	112
9	80	113
10	81	119
20	82	120
21	83	121
22	84	130
23	85	131
46	86	136
48	88	140
49	97	149
50	98	150
51	99	151
52	100	152
53	101	153
		163
		164
		165
		166
		167
		168

Table 4. Rain gage sites eliminated for having less than 60% pasture in the surrounding 1 sq. km.

ORIGINAL PAGE IS
OF POOR QUALITY



Figure 11. Day/night temperature difference greymap of the Washita Watershed area for October 16 and 17

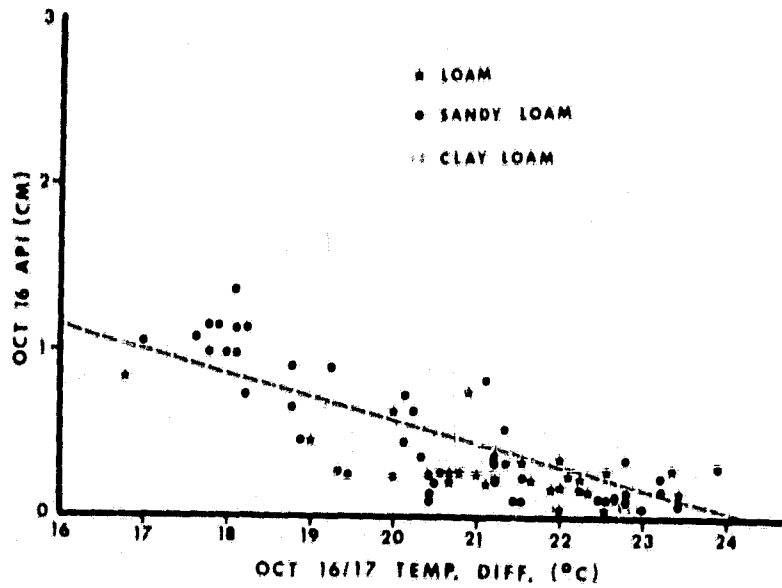


Figure 12. Oct. 16/17 day/night temperature differences versus API conditions ($R^2=0.25$)

pixels (1 square kilometer). We also had to eliminate several points along the southern part of the watershed as the southern image boundary cut through the center of the watershed (Figure 13). Surface temperatures were cool in the north part of the watershed on the 12th and were uniform on the night of the 15th (Figure 14). The October 12/October 15 day/night temperature differences correlated well with API in (Figure 15). Coefficient of determination values were quite high ($R^2=.76$) thus indicating that pasture day/night temperature differences were strongly related to API conditions 3-4 days after the storm. The relationship decreased as the period between the storm and thermal measurements increased.

In spite of the good relationship, October was the only period in 1978 when HCMM was able to collect a reasonable amount of day/night thermal data. Excessive cloud cover over the watershed was the main reason. Alternate satellite data (GOES) during 1978 was also analyzed; however, the spatial resolution (8km) was too large to delineate surface features.

Day/Day Temperature Differences vs API

On July 21, 1978 a storm passed over parts of the watershed. Some areas received as much as 6 cm, while other areas received none (Figure 16). Moisture conditions before the storm were quite dry; API values were approximately 0.5 cm throughout the watershed. HCMM collected day IR data over the site on July 13, (ID A-A0078-19560), July 24 (ID A-A0089-20000), and July 29 (ID A-A0094-19580); however, no night infrared data was available during this period due to excessive cloud cover. An alternate normalization factor besides night

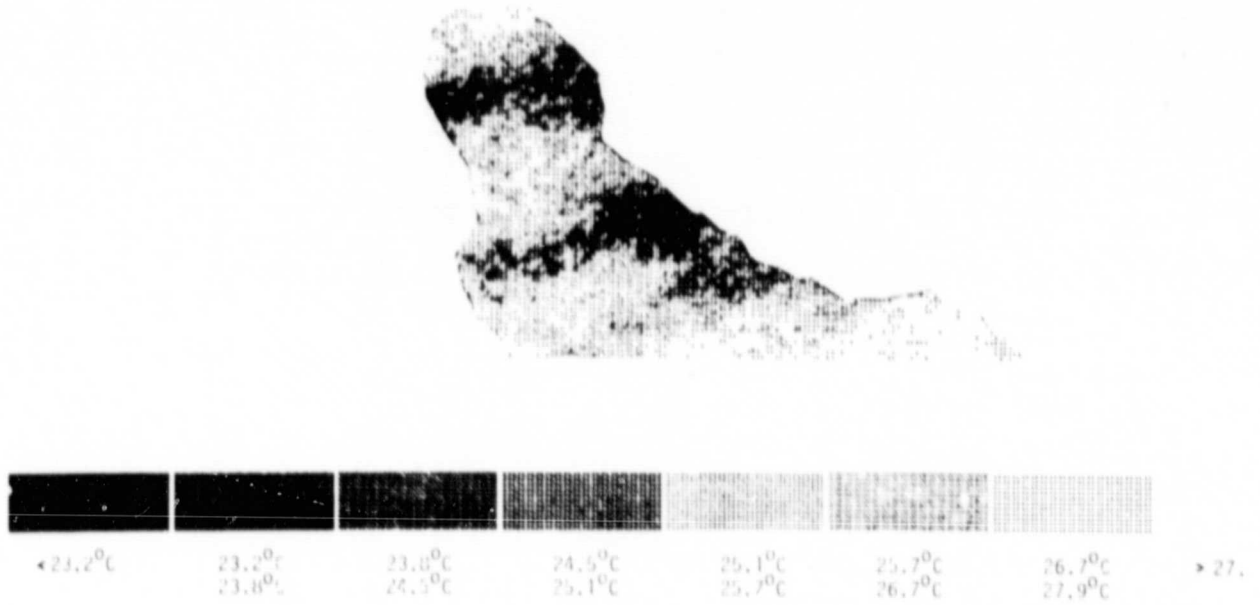


Figure 13. October 12 day IR greymap, the southern part of the watershed was not included with the digital (CCT) data

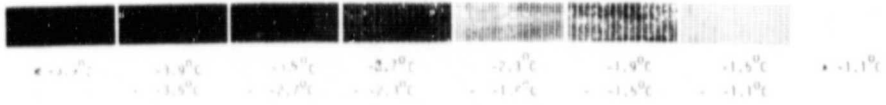


Figure 14. October 15 night IR greymap of the Washita Watershed area

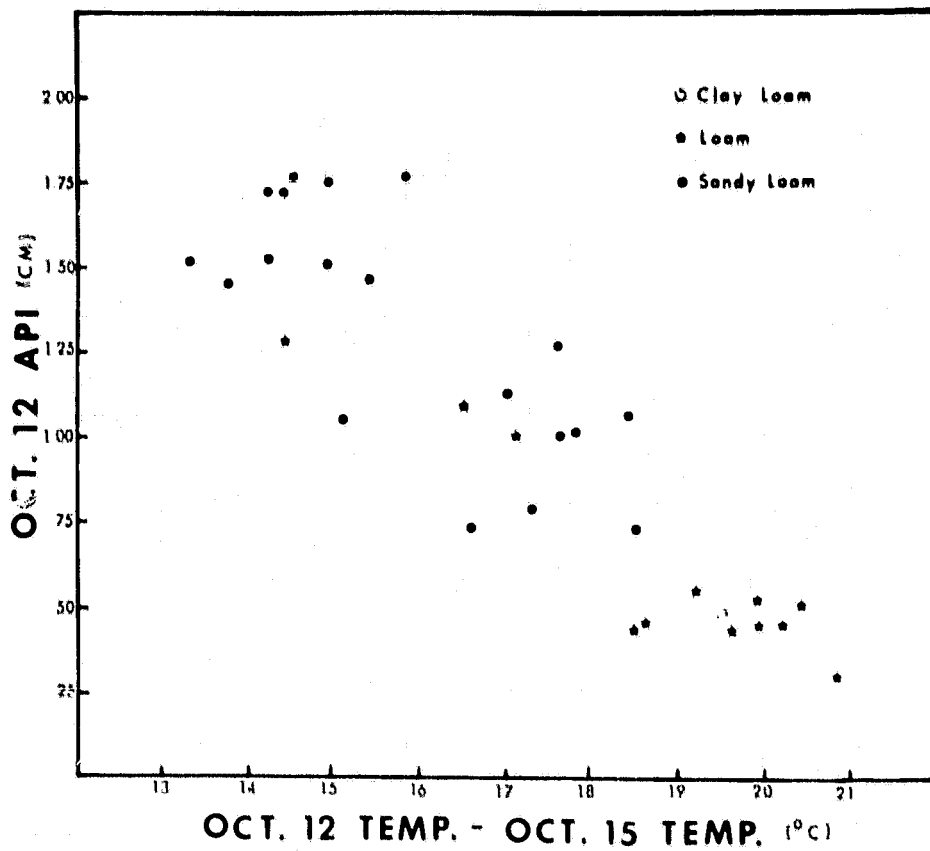


Figure 15. Oct 12/15 day/night temperature differences versus API conditions ($R^2=0.76$)



Figure 16. Rainfall contour map of the July 21, 1978 storm which passed over parts of the watershed area

IR data was needed. One possible means was to calculate day/day surface temperature differences. The reasoning can be explained through the energy balance equation:

$$R_n = LE - H - G \quad (7)$$

where R_n is net radiation, LE is latent heat flux, and H is sensible heat flux, and G is soil heat flux (Geiger, 1950). Given the same radiative difference between net radiation and sensible heat transfer ($R_n - H$) on two days, the date having higher moisture contents would have more energy apportioned to LE than G , the variable which determines soil temperature. As a result wetter areas would appear cool compared to dry areas. By determining the temperature difference between wet and dry thermal IR scenes, areas which have become wetter will have a larger day/day temperature difference compared to drier areas. The only constraints would be to develop a technique to normalize net radiation between dates and correct for atmospheric absorption. One way to normalize net radiation would be to use air temperature differences, a rough indication of net radiation differences between clear days. This technique and the atmospheric correction, as calculated from lake temperatures, were used to correct surface temperature data.

With this idea, the July 13 thermal data was selected as the dry, reference date before the storm. Because the three dates were within 17 days of each other and cloud cover was similar, each day had approximately the same amount of net radiation. Except for some small cumulus clouds, surface temperatures on July 13 were quite uniform (Figure 17).

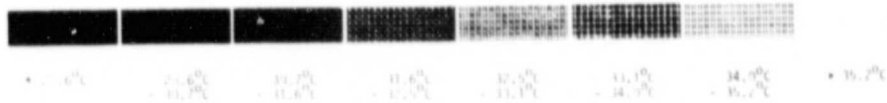


Figure 17. Thermal IR greymap of the Washita Watershed area on July 13, 1978

ORIGINAL PAGE IS
OF POOR QUALITY

The day/day temperature differences were checked by analyzing differences between actual lake temperature at Ft. Cobb Reservoir and Lake Ellsworth--two lakes near the watershed--and HCMM apparent lake temperatures for each pass date. The HCMM and actual lake temperature differences on July 24 were less than 0.5°C. For July 29 the HCMM and actual lake temperature difference was 6°C. Both differences were very similar (within 1-2°C) to the atmospheric corrections as calculated by RADTRA, the atmospheric correction model provided by NASA/GSFC. The atmospheric correction and net radiation normalization (using air temperature differences) were then added, giving the total surface temperature correction. The total correction for the July 13/July 24 comparison was 5°C, and for the July 13/July 29 comparison, 6°C.

On July 24, a cool, dark band extended from southwest to northeast across the watershed (Figure 18). The band is still evident even on July 29 (Figure 19). In both cases the cool band followed the area of heaviest rainfall across the watershed.

Transects were located between points A and B (Figures 18 and 19) across the storm track. Surface temperatures and API values were then compared along the transects. Figures 20 and 21 indicated high API values were related to lower temperatures and vice versa. Consequently, day thermal IR data alone located areas of relatively high or low moisture stress.

The July 24/July 13 day/day temperature differences were highly related to API (Figure 22). The coefficient of determination, 0.58, improved to 0.68 if we set API values equal to zero for the areas

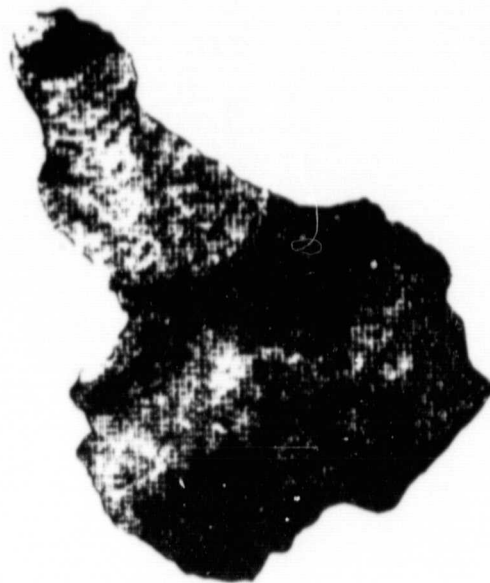


Figure 18. Thermal IR greymap of the Washita watershed area on July 24, 1978

ORIGINAL PAGE IS
OF POOR QUALITY

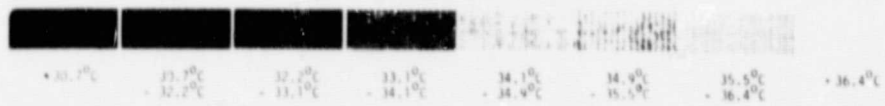
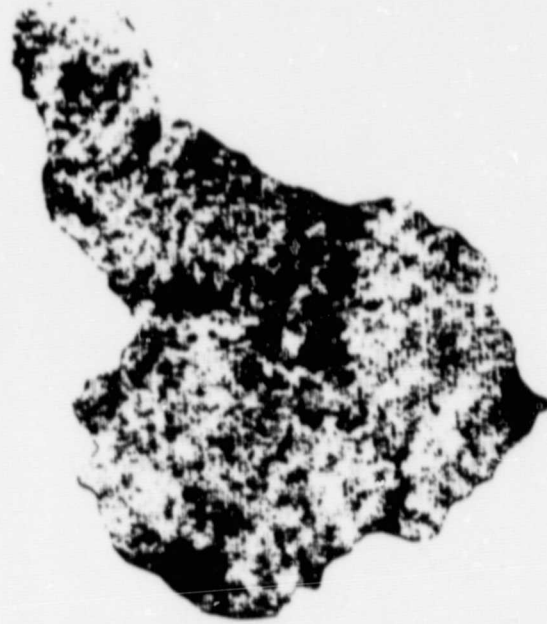


Figure 19. Thermal IR greymap of the Washita Watershed area on July 29, 1978

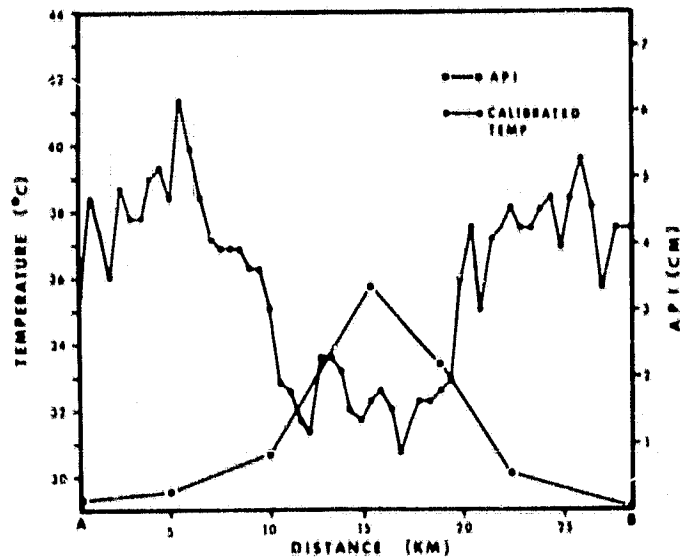


Figure 20. Surface temperature and API as a function of distance along the transect A-B on July 24, 1978

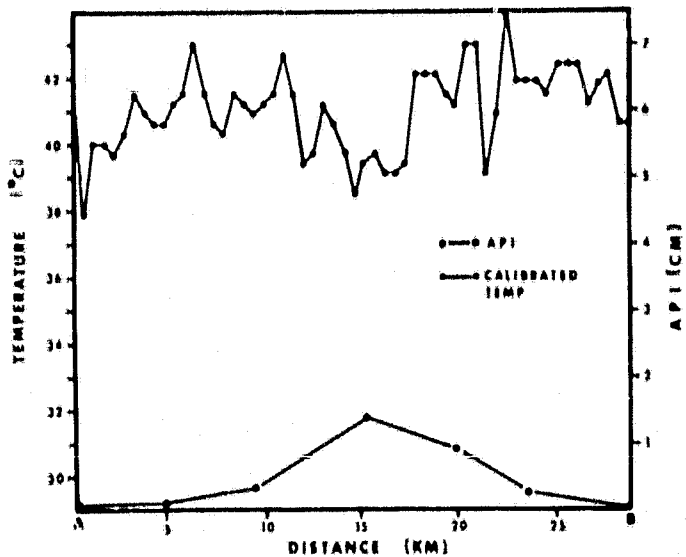


Figure 21. Surface temperatures and API as a function of distance along transect A-B on July 29, 1978

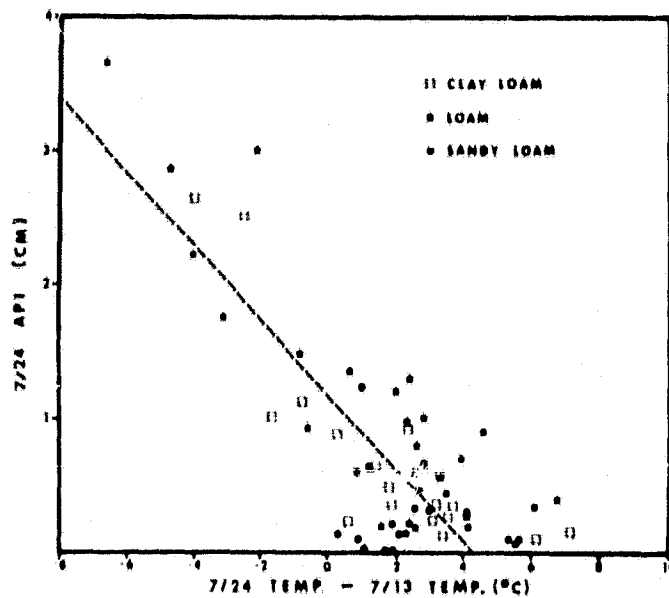


Figure 22. July 24/July 13 day/day temperature differences versus API conditions on July 24 ($R^2=0.68$)

having a temperature difference greater than 5°C and determined a new regression line for the rest of the data. The calculated regression line is plotted on Figure 22. A negative temperature difference inferred that July 24 surface temperatures were cooler than July 13 temperatures.

Results of the July 29/July 13 temperature versus API relationship were not as highly correlated (Figure 23). The coefficient of determination decreased to 0.25 indicating that other factors--temperature variability due to land use variation--are again influencing temperature variation. Also, day/day temperature differences may estimate API values above 1 cm for a period of only about 7 days. The regression line as calculated for the July 24/13 relationship was plotted as a dotted line in Figure 23. A few points with API estimates above 1 cm were close to the July 24/13 relationship, indicating the normalization technique appeared to work well in this case.

Comparison of the Two Techniques

Since both day/night and day/day temperature differences were highly related to API conditions, we attempted to compare results from the two techniques for the same storm. A comparison was made between the October 16/17 and October 12/15 day/night images with the October 17/August 31 (ID A-A0127-20000) and October 12/August 31 day/day images. API values from October 12 through 17 ranged from 0.20 to 3.0 cm and for August 31 values were approximately .30 cm. Since there is a 40-50 day difference, we compared the temperature differences to API differences. The data processing procedure was

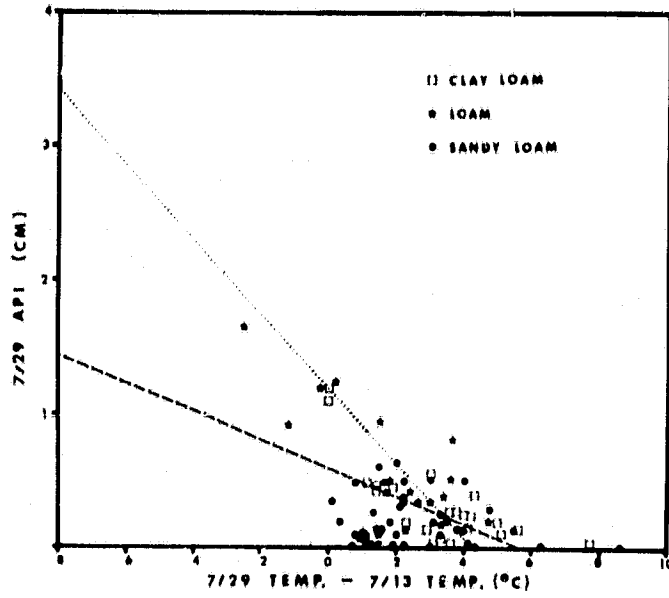


Figure 23. July 29/July 13 day/day temperature differences versus July 29 API ($R^2=0.25$)

the same as described in the previous sections. Total atmospheric corrections proved to be quite large--approximately 9°C through the period.

On August 31 surface temperatures were quite uniform having a range of only 6°C (Figure 24). The day/day and day/night results for October 12/August 31 and October 12/October 15 (ID A-A172-08350) periods were well correlated with API differences (Figures 25 and 15). The coefficient of determination for the day/day relationship was 0.57, thus indicating that the day/night relationship was slightly better than the day/day relationship, assuming registration errors are the same for both techniques.

The day/day and day/night results for October 17/August 31 and October 16/17 were not as strongly related to API (Figures 26 and 12). Note that the day/day relationship had an R^2 value of 0.43 while the day/night relationship had a value of 0.25. These values suggest that API estimates were reasonably accurate up to approximately one week after the storm. After that period the relationship degraded as other variables which affect surface temperature variability predominate.

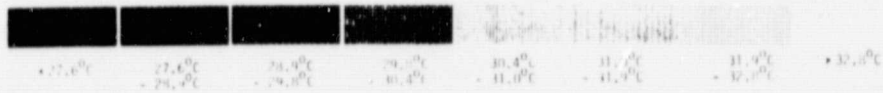
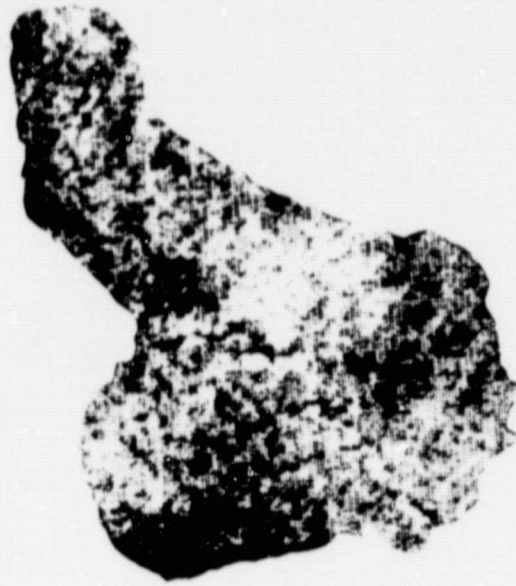


Figure 24. Thermal IR greymap of the Washita Watershed area on August 31, 1978

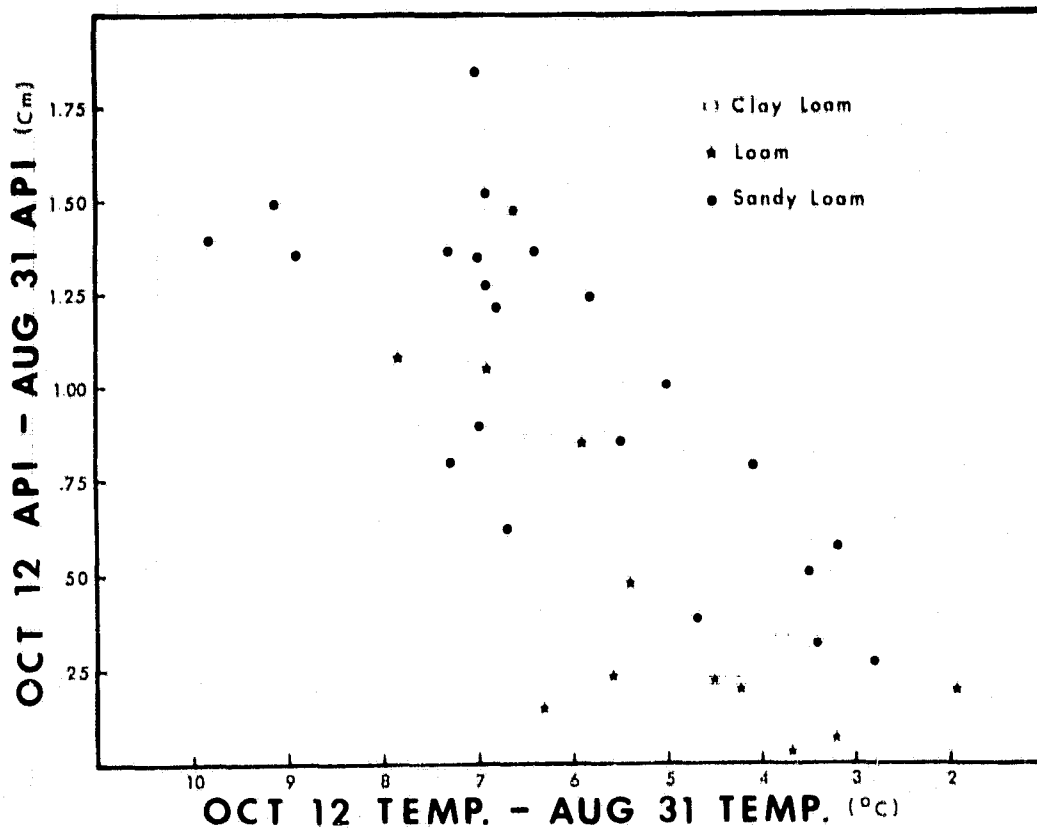


Figure 25. October 12/August 31 day/day temperature difference versus API differences between the same two dates ($R^2=0.57$)

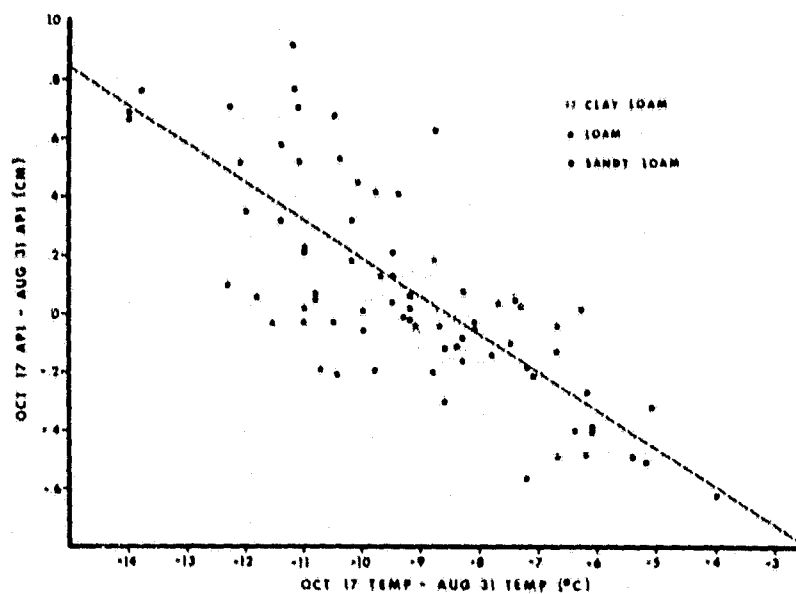


Figure 26. October 17/August 31 day/day temperature differences versus API differences between the same days ($R^2=0.43$)

CONCLUSIONS

From thermal measurements collected during the contract period--aircraft and HCMM--we found 1) canopy temperatures were accurately measured remotely, 2) pasture surface temperature differences detected relative soil moisture (API) differences (the coefficient of determination is as high as 0.76), 3) pasture surface temperatures were related to stress (low API) in nearby cash-crop fields (i.e. wheat), and 4) no relationship was developed between final yield differences, thermal infrared data, and soil moisture stress at critical growth stages due to a lack of thermal data at critical growth stages (the only data collected was aircraft data in May 1978). Bad weather was the major factor limiting acquisition of adequate amounts of satellite data during critical growth stages--especially night IR data. Also, 12- to 36- hour passes were too infrequent (every 7 to 16 days). Chances of obtaining day/night IR data improve with more frequent passes.

Reacting to the problem of inadequate numbers of day/night IR data sets, we analyzed day/day temperature differences. Data was normalized using lake surface temperatures (to compensate for atmospheric absorption) and air temperature (to compensate for net radiation differences). The present normalization technique adequately calculated relative API differences for one storm, but a better normalization technique needs to be developed to compare API differences between different storms (i.e., July 24 and October 12 storms). Results indicated that the day/day relationship is almost as good as the day/night relationship. The relationships hold out for

approximately 7 days after the storm when other factors besides soil moisture influence the surface temperature variations across the scene. One such factor is incomplete canopy cover. Heilman and Moore (1980) eliminated this factor by developing an empirical technique to estimate surface soil moisture from surface temperatures of partial canopy covers. Other techniques also need to be developed to eliminate the thermal influence of other factors. Given the thermal/API relationship up to 7 days after a storm the 16-day HCMM overpass interval is inadequate. More frequent passes are required.

We have only begun to understand thermal patterns as related to highly stressed and non-stressed areas. Many of the HCMM images discussed in this report display variations in soil moisture (API and precipitation patterns as small as 5 km wide). Such results are extremely valuable as inputs to various models (agricultural, yield, soil water budget) requiring high spatial resolution data. Further analysis of satellite thermal IR data may aid in the development of soil moisture "maps" of a given area.

BIBLIOGRAPHY

- Blanchard, B. J. 1978. Personal Communication.
- Campbell, G. S., 1977. An introduction to environmental biophysics. Springer-Verlag. New York.
- Fuchs, M. and G. B. Tanner. 1966. Infrared thermometry of vegetation. Agron. J., 58:597-601.
- Gardner, B. R. 1979. Plant and canopy temperatures in corn as influenced by differential moisture stress. M. S. Thesis. University of Nebraska.
- Geiger, R. 1950. The climate near the ground. Harvard University Press. Cambridge, Mass.
- Harlan, J. C., W. E. Boyd, C. Clark, S. Clarke, O. C. Jenkins. 1978. Rangeland resource evaluation from Landsat. Progress Report RSC 3715-2. Texas A&M University. College Station, TX.
- Heilman, J. L. and D. G. Moore. 1980. Thermography for estimating near-surface soil moisture under developing crop canopies. J. Appl. Met. 19:324-328.
- Jackson, R. D., R. J. Reginato, and S. B. Idso. 1977. Wheat canopy temperature: a practical tool for evaluating water requirements. Water Resources Research 13:651-656.
- NOAA. 1980. Climatic data of the U. S.--(Oklahoma). U.S. Commerce Dept.
- Robins, J. S. and C. E. Domingo. 1962. Moisture and nitrogen effects on irrigated spring wheat. Agron. J. 54:135-138.